Carrier Transport Properties of Monodisperse Glassy-Nematic Oligofluorenes in Organic Field-Effect Transistors

Takeshi Yasuda, Katsuhiko Fujita, and Tetsuo Tsutsui*

Department of Applied Science for Electronics and Materials, Graduate School of Engineering Sciences, Kyushu University, Kasuga, Fukuoka 816-8580, Japan

Yanhou Geng, Sean W. Culligan, and Shaw H. Chen*

Department of Chemical Engineering and Laboratory for Laser Energetics, Center for Optoelectronics and Imaging, University of Rochester, 240 East River Road, Rochester, New York 14623-1212

Received August 31, 2004. Revised Manuscript Received October 30, 2004

A heptafluorene, F(Pr)5F(MB)2, a dodecafluorene, F(MB)10F(EH)2, and poly(9,9′-dioctylfluorene), PFO, were used to prepare field-effect transistors. Monodomain and polydomain glassy-nematic films as well as glassy-amorphous films were prepared for the measurement of hole mobility. In a monodomain film, the $\mu_{\|}$ value is determined by the chain length in oligofluorene and the persistence length in polyfluorene. Mobility in a polydomain film lies between $\mu_{\|}$ and $\mu_{\perp}$ of a monodomain film. Amorphous films possess the lowest mobility of all presumably because of the geometric and energetic disorder. The OFET containing a monodomain glassy-nematic film of F(MB)10F(EH)2 exhibits a field-effect mobility of 0.012 cm^2/Vs with an on/off current ratio of 1.0×10^4, a substantial improvement over a monodomain glassy-nematic film of PFO.

Introduction

Since the late 1980s π-conjugated polymers have been actively pursued for photonics and electronics, such as field-effect transistors (FETs),[1−3] light-emitting diodes,[4,5] solar cells,[6] and solid-state lasers.[7] Typically purified by precipitation, conjugated polymers are characterized by a distribution in chain length and chemical composition. In contrast, monodisperse conjugated oligomers are structurally uniform with superior chemical purity accomplished by recrystallization or column chromatography.[8−12] For instance, monodisperse oligofluorenes are capable of self-organization into uniaxially aligned, defect-free films for the realization of strongly polarized and highly efficient organic electroluminescence at a performance level consistently better than that of polymer analogues.[13−16] Furthermore, spin-cast glassy-nematic films comprising monodisperse oligofluorenes are stable against recrystallization when left at room temperature for over two years. The ability to resist crystallization from the glassy-nematic state is essential to the prevention of device failure. In the absence of chain entanglements, bends, or kinks, all acting as charge traps, monodisperse oligofluorenes are expected to yield a high charge carrier mobility. From a device perspective, a highly anisotropic mobility suppresses cross-talk in logic circuits and pixel switching elements in displays.

There has been a recent surge of interest in organic semiconductors with high carrier mobility in the broad context of organic electronics through ordering at the molecular level, as in single-crystalline,[17,18] polycrystalline,[19−24] and vitrified liquid-crystalline films.[25−29] Although mobility exceeding that of amorphous silicon has been achieved, difficulties with film

* To whom correspondence should be addressed. E-mail: tsuigz@mbox.nc.kyushu-u.ac.jp (T.T.); shch@lle.rochester.edu (S.H.C.).

(1) Tsumura, A.; Koezuka, K.; Ando, T. *Appl. Phys. Lett.* **1986**, *49*, 1210.
(2) Meijer, E. J.; de Leeuw, D. M.; Setayesh, S.; van Veenendaal, E.; Huisman, B.-H.; Blom, P. W. M.; Hummelen, J. C.; Scherf, U.; Klapwijk, T. M. *Nat. Mater.* **2003**, *2*, 678.
(3) Horowitz, G. *J. Mater. Res.* **2004**, *19*, 1946.
(4) Burroughes, J. H.; Bradley, D. D. C.; Brown, A. R.; Marks, R. N.; Mackay, K.; Friend, R. H.; Burnss, P. L.; Holmes, A. B. *Nature* **1990**, *347*, 539.
(5) Mitschke, U.; Bäuerle, P. *J. Mater. Chem.* **2000**, *10*, 1471.
(6) Brabec, C. J.; Sariciftci, N. S.; Hummelen, J. C. *Adv. Funct. Mater.* **2001**, *11*, 15.
(7) McGehee, M. D.; Heeger, A. J. *Adv. Mater.* **2000**, *12*, 1655.
(8) Lee, S. H.; Tsutsui, T. *Thin Solid Films* **2000**, *363*, 76.
(9) Lee, S. H.; Nakamura, T.; Tsutsui, T. *Org. Lett.* **2001**, *3*, 2005.
(10) Geng, Y.; Culligan, S. W.; Trajkovska, A.; Wallace, J. U.; Chen, S. H. *Chem. Mater.* **2003**, *15*, 542.
(11) Meng, H.; Zheng, J.; Lovinger, A. J.; Wang, B. C.; Van Patten, P. G.; Bao, Z. *Chem. Mater.* **2003**, *15*, 1778.
(12) Meng, H.; Bao, Z.; Lovinger, A. J.; Wang, B. C.; Mujsce, A. M. *J. Am. Chem. Soc.* **2001**, *123*, 9214.
(13) Whitehead, K. S.; Grell, M.; Bradley, D. D. C.; Inbasekaran, M.; Woo, E. P. *Synth. Met.* **2000**, 111−112, 181.
(14) Culligan, S. W.; Geng, Y.; Chen, S. H.; Klubek, K.; Vaeth, K. M.; Tang, C. W. *Adv. Mater.* **2003**, *15*, 1176.
(15) Geng, Y.; Chen, A. C. A.; Ou, J. J.; Chen, S. H.; Klubek, K.; Vaeth, K. M.; Tang, C. W. *Chem. Mater.* **2003**, *15*, 4352.
(16) Chen, A. C. A.; Culligan, S. W.; Geng, Y.; Chen, S. H.; Klubek, K. P.; Vaeth, K. M.; Tang, C. W. *Adv. Mater.* **2004**, *16*, 783.
(17) Sundar, V. C.; Zaumseil, J.; Podzorov, V.; Menard, E.; Willett, R. L.; Someya, T.; Gershenson, M. E.; Rogers, J. A. *Science* **2004**, *303*, 1644.
(18) Mas-Torrent, M.; Durkut, M.; Hadley, P.; Ribas, X.; Roviro, C. *J. Am. Chem. Soc.* **2004**, *126*, 984.
(19) Sirringhaus, H.; Brown, P. J.; Friend, R. H.; Nielsen, M. M.; Bechgaard, K.; Langeveld-Voss, B. M. W.; Spiering, A. J. H.; Janssen, R. A. J.; Meijer, E. W.; Herwig, P.; de Leeuw, D. M. *Nature* **1999**, *401*, 685.
(20) Mushrush, M.; Facchetti, A.; Lefenfeld, M.; Katz, H. E.; Marks, T. J. *J. Am. Chem. Soc.* **2003**, *125*, 9414.
(21) Melucci, M.; Gazzano, M.; Barbarella, G.; Cavallini, M.; Biscarini, F.; Maccagnani, P.; Ostoja, P. *J. Am. Chem. Soc.* **2003**, *125*, 10266.
(22) Dimitrakopoulos, C. D.; Malenfant, P. R. L. *Adv. Mater.* **2002**, *14*, 99.
(23) Fichou, D. *J. Mater. Chem.* **2000**, *10*, 571.
(24) Bao, Z.; Rogers, J. A.; Katz, H. E. *J. Mater. Chem.* **1999**, *9*, 1895.

10.1021/cm048532s CCC: $30.25
Published on Web 12/30/2004

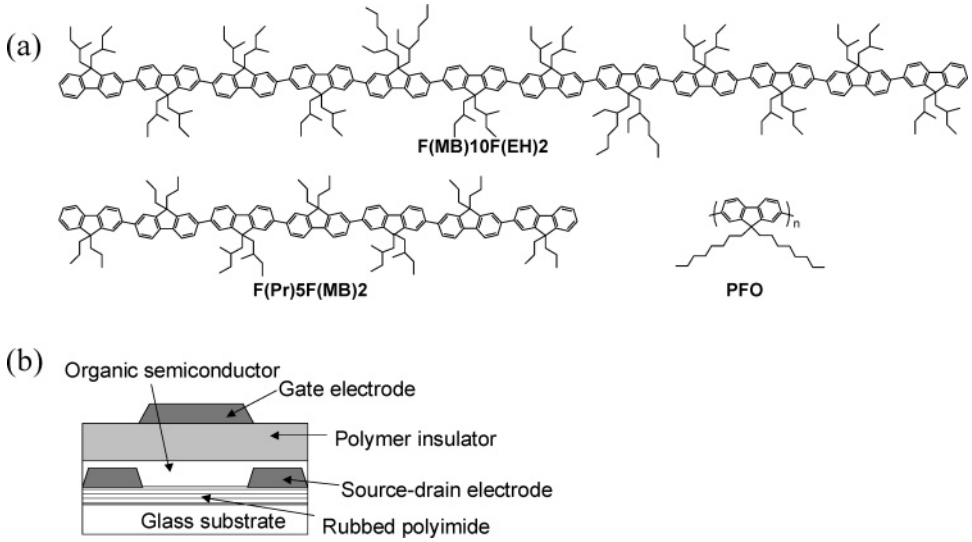

Figure 1. (a) Molecular structures of the organic semiconductors. (b) Schematic diagram of the organic field-effect transistors used in this study.

processing, reproducibility, and air stability remain to be overcome. Single-crystalline films are limited to a small area. Polycrystalline films can be prepared across a large area, but mobility varies with chemical impurities, crystal grain size, crystallographic defects, and the orientation and order of π-stacks. Thermotropic poly(9,9′-dioctylfluorene), PFO, and poly(9,9′-dioctyl-fluorene-*co*-bithiophene), F8T2, have been attempted to address the issue of processability into large-area films without grain boundaries.[25−27] The present study takes advantage of molecular self-assembly of monodisperse oligofluorenes for the preparation of FETs. Glassy nematic oligofluorenes have been explored for two reasons: the molecular order prevailing in the liquid crystal state can be frozen into the solid state by cooling across the glass transition temperature, and monodomain glassy liquid-crystal films can be readily prepared across a large area. Furthermore, a strong π-orbital interaction prevails in monodisperse oligofluorene films, as evidenced by the pronounced hypochromism (see Figure 4a of ref 10). Hence, monodomain glassy-nematic films of oligofluorenes have the intrinsic merit of interchain π-orbital interaction without grain boundaries. Here we report on the hole mobility in monodomain and polydomain glassy-nematic films, as well as glassy-amorphous films comprising monodisperse oligofluorenes and poly(9,9′-dioctylfluorene), to investigate the effects on mobility of the oligomer's chain length, the polymer's persistence length, and the film morphology.

Experimental Section

Clean glass substrates were spin-coated with a polyamic acid precursor solution (Nissan SUNEVER150) and then baked at 280 °C for 1 h to achieve full imidization. The resultant polyimide (PI) film with thickness of 400 nm was uniaxially rubbed with a velvet cloth. Atomic force microscopy (AFM, Nanopics1000, Seiko instruments Inc.) images revealed that the rubbed PI surface had a root-mean-square roughness (RMS) of 5.40 nm. Films with a thickness ranging from 40 to 60 nm of F(Pr)5F(MB)2, F(MB)10F-(EH)2, and PFO, as depicted in Figure 1a, were prepared by spin-coating from 0.5 wt % solutions in chloroform at a spin rate of 1500 rpm. The surface of spin-coated PFO film on the rubbed PI had RMS of 4.05 nm. The synthesis and purification of oligofluorenes were as described previously,[10] and PFO with a weight-average molecular weight of 140 000 g/mol and a polydispersity factor of 1.9 was used as received from American Dye Source, Inc. On the basis of heating scans of differential scanning calorimetry, F(Pr)5F(MB)2 has a glass transition temperature, T_g, at 149 °C and a nematic-to-isotropic transition temperature, T_c, at 366 °C; F(MB)10F(EH)2 has a T_g at 123 °C and a T_c beyond 375 °C; and PFO has a T_g at 75 °C and a T_c at 285 °C. The organic semiconducting films were aligned by thermal annealing under N_2 atmosphere at 160, 140, and 220 °C for F(Pr)5F(MB)2, F(MB)-10F(EH)2, and PFO, respectively, over a period of $^1/_2$ h followed by quenching to room temperature. Note that thermal annealing was performed at a temperature slightly above T_g for oligofluorenes, and substantially above T_g for polyfluorene because of its relatively high melt viscosity. The resultant monodomain glassy-nematic films were characterized by UV−vis−NIR spectrophotometry (UV-3150, Shimazu) for the determination of orientational order parameter.

OFETs were fabricated on rubbed and unrubbed PI with a top gate geometry shown in Figure 1b. The 40-nm-thick gold source-drain electrodes with an interdigitated configuration were deposited through a shadow mask. The channel length L and width W were 75 μm and 5 mm, respectively. Films of F(Pr)5F(MB)2, F(MB)-10F(EH)2, and PFO were formed by spin-coating. Monodomain glassy-nematic films were prepared following the same procedure as described above. On unrubbed PI, polydomain glassy-nematic and glassy-amorphous films emerged with and without thermal annealing, respectively. On top of the organic semiconducting films, poly-chloro-*p*-xylylene (diX-C, Daisankasei Co. Ltd.) was deposited by CVD with a thickness ranging from 500 to 800 nm to serve as a gate insulator for OFETs.[30,31] The dielectric capacitance of the

(25) Redecker, M.; Bradley, D. D. C.; Inbasekaran, M.; Woo, E. P. *Appl. Phys. Lett.* **1999**, *74*, 1400.
(26) Sirringhaus, H.; Wilson, R. J.; Friend, R. H.; Inbasekaran, M.; Wu, W.; Woo, E. P.; Grell, M.; Bradley, D. D. C. *Appl. Phys. Lett.* **2000**, *77*, 406.
(27) Heeney, M.; Bailey, C.; Giles, M.; Shkunov, M.; Sparrowe, D.; Tierney, S.; Zhang, W.; McCulloch, I; *Macromolecules* **2004**, *37*, 5250.
(28) O'Neill, M.; Kelly, S. M.; *Adv. Mater.* **2003**, *15*, 1135.
(29) McCulloch, I.; Zhang, W.; Heeney, M.; Bailey, C.; Giles, M.; Graham, D.; Shkunov, M.; Sparrowe, D.; Tierney, S. *J. Mater. Chem.* **2003**, *13*, 2436.
(30) Yasuda, T.; Fujita, K.; Nakashima, H.; Tsutsui, T. *Jpn. J. Appl. Phys., Part 1* **2003**, *42*, 6614.
(31) Yasuda, T.; Fujita, K.; Tsutsui, T. *Proc. SPIE* **2003**, *5217*, 202.

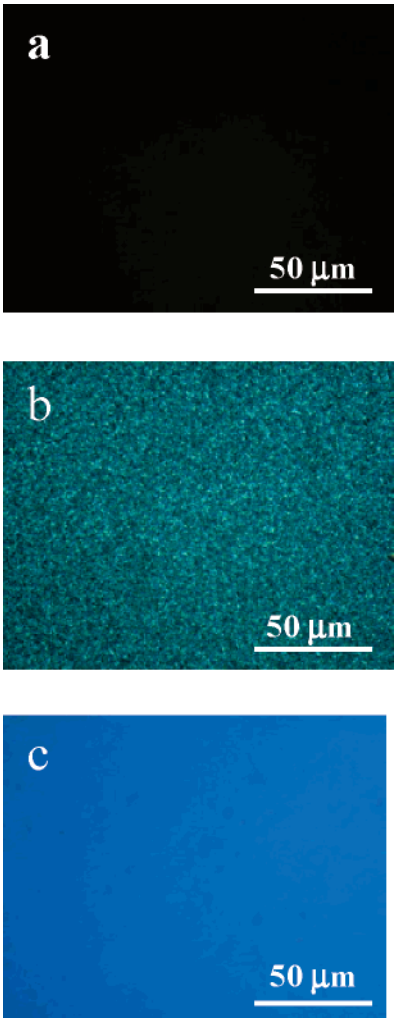

Figure 2. Polarizing optical micrographs of (a) a glassy-amorphous film; (b) a polydomain glassy-nematic film; and (c) a monodomain glassy-nematic film of F(Pr)5F(MB)2 with a thickness ranging from 40 to 60 nm.

insulating layer per unit area C_i ranged from 5.68 to 3.55 nF/cm^2. The OFETs were completed by depositing a gold gate electrode through a shadow mask to form a 5-mm-wide and 30-nm-thick line as a gate electrode. The film thickness was determined with a Sloan Dektak 3 profilometer in all cases. All the OFETs were temporarily exposed to air prior to characterization by an Agilent 4156C precision semiconductor parameter analyzer in a vacuum atmosphere. The electric parameters were estimated using a standard analytic theory of MOSFET according to the following equation:

$$I_{D,sat} = \frac{WC_i}{2L}\mu(V_G - V_T)^2$$

where $I_{D,sat}$ is the saturation drain current, V_T is the threshold voltage, V_G is the gate voltage, and μ is the field-effect mobility. The highest occupied molecular orbital (HOMO) energy levels were determined by photoemission spectroscopy (AC-2, Rikenkeiki) using spin-cast films on an indium−tin-oxide electrode.

Results and Discussion

Polarizing optical micrographs of glassy-amorphous, polydomain glass-nematic, and monodomain glassy-nematic films encountered in this work are illustrated with spin-cast films of F(Pr)5F(MB)2 in Figure 2. An amorphous film appears to be dark at all orientations of the rubbing direction (a), a polydomain nematic film contains fine threaded textures (b), and a monodomain nematic film is devoid of disclinations (c). Anisotropic absorption spectra are compiled in Figure 3 for monodomain glassy-nematic films consisting of (a) F(Pr)-5F(MB)2, (b) F(MB)10F(EH)2, and (c) PFO. The absorption dichroic ratio R_{abs} is defined as $A_{\parallel}/A_{\perp}$, the absorbance parallel over that perpendicular to the nematic director as defined by the rubbing direction on the polyimide alignment layer. The values of the orientational order parameter, $S_{abs} = (R_{abs} - 1)/(R_{abs} + 2)$, are also included in Figure 3. Note the marginal increase in the orientational order parameter from heptafluorene (0.77) to dodecafluorene (0.79), but the substantial decrease to PFO (0.66), indicating a relative ease of aligning oligomers under the processing conditions stated in the Experimental Section. In contrast, vanishing S_{abs} values were observed for polydomain glassy-nematic and glassy-amorphous films of all three materials.

Shown in Figure 4a are the source-drain current−voltage (I_D−V_D) relationships for a V_G from 0 to −70 V for an OFET comprising a monodomain F(MB)10F(EH)2 film on a PI layer rubbed parallel to the direction of current flow. Above the threshold voltage, the field-effect mobility can be calculated from the slope of the linear portion of $|I_{D,sat}|^{1/2}$ as a function of V_G. From the plot in Figure 4b, a field-effect mobility of 0.012 cm^2/Vs emerged with a threshold voltage of −43 V and an on/off ratio of 1.0×10^4. In the same device structure, a monodomain glassy-nematic film of PFO yielded a mobility of 5.8×10^{-3} with an on/off ratio of 7.4×10^3. The HOMO energy levels of F(MB)10F(EH)2 and PFO were found to be 5.9 and 5.8 eV, respectively, indicating little difference in hole injection barrier from Au (5.1 eV). A simulation of OFETs has shown that a large injection barrier from source-drain electrodes to organic semiconductor causes a large decrease in field-effect mobility.[32] In view of the nearly identical hole injection barrier, a higher field-effect mobility of F(MB)10F(EH)2 than that of PFO can be attributed to the difference of hole transport properties in these two materials. The linear plot of I_D versus V_D for the OFET comprising a glassy-amorphous F(MB)10F(EH)2 film for a V_G from 0 to −70 V is presented Figure 5a. The plot in Figure 5b furnished a field-effect mobility of 1.5×10^{-5} cm^2/Vs with a threshold voltage of −23 V and an on/off ratio of 37.

Figure 6 shows the transfer characteristics (at a drain voltage of −100 V) of OFETs with channel parallel (open circles) and perpendicular (open squares) to the nematic director in a monodomain glassy-nematic film of F(MB)-10F(EH)2. The characteristics of polydomain glassy-nematic (open triangles) and glassy-amorphous (crosses) F(MB)10F-(EH)2 films are also shown. It is clear that thermal annealing led to a significant enhancement in the drain current. The results on the field-effect mobility for all films of F(MB)-10F(EH)2, F(Pr)5F(MB)2, and PFO are summarized in Table 1, where $\mu_{\parallel}$ and $\mu_{\perp}$ represent mobility parallel and perpendicular, respectively, to the nematic director in a monodomain glassy-nematic film, and $\mu_{\times}$ and μ_a represent that of a polydomain glassy-nematic and a glassy-amorphous film, respectively.

(32) Bolognesi, A.; Di Carlo, A.; Lugli, P. *Appl. Phys. Lett.* **2002**, *81*, 4646.

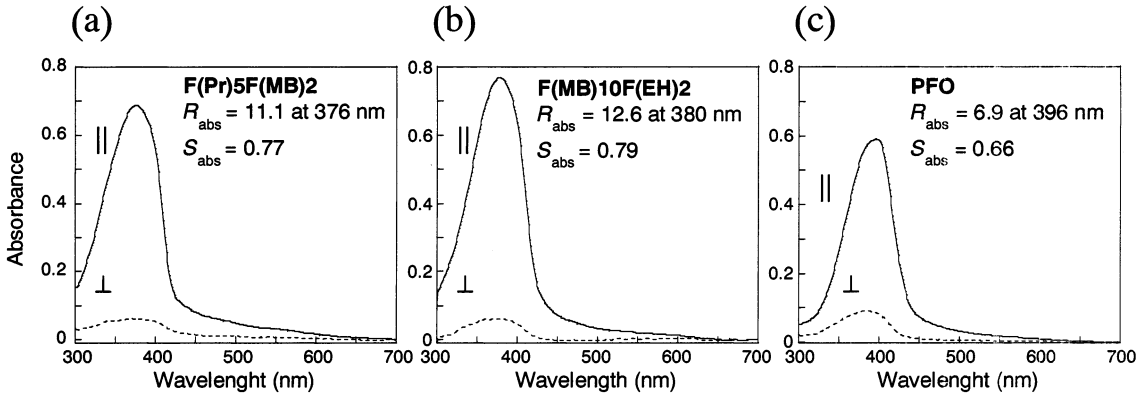

Figure 3. Polarized absorption spectra of 40−60-nm-thick monodomain glassy-nematic films parallel (||) and perpendicular (⊥) to the rubbing direction.

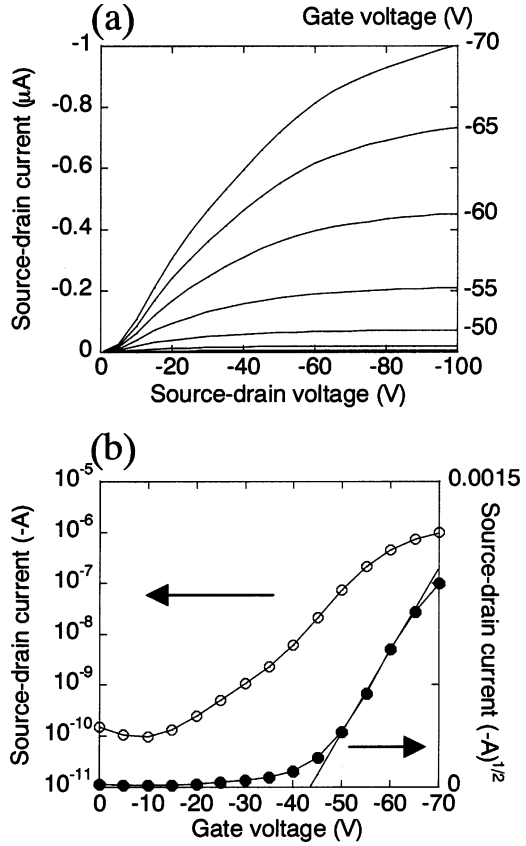

Figure 4. (a) Plots of the I_D versus V_D at various V_G values for the OFET consisting of a monodomain glassy-nematic F(MB)10F(EH)2 film. (b) Plots of the I_D (left) and square root of I_D (right) versus V_G at $V_D = -100$ V.

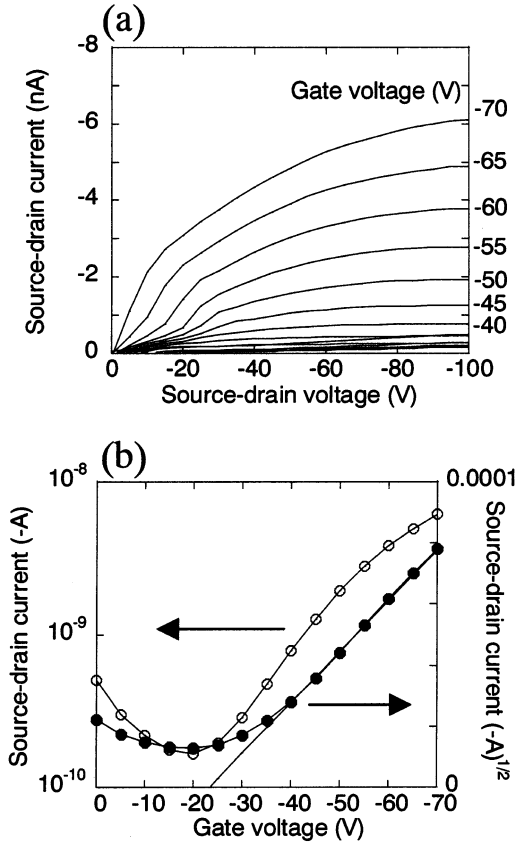

Figure 5. (a) Plots of the I_D versus V_D at various V_G values for the OFET consisting of a glassy-amorphous film of F(MB)10F(EH)2. (b) Plots of the I_D (left) and square root of I_D (right) versus V_G at $V_D = -100$ V.

As shown in Table 1, the field-effect mobilities of monodomain glassy-nematic films are anisotropic, viz. charge transport parallel to the backbone orientation is greater than that perpendicular. Anisotropic charge transport has also been reported for a F8T2 film aligned by thermal annealing[26] or a regioregular poly(3-dodecylthiophene), P3DDT, film aligned by drawing method.[33] The anisotropy factor, $\mu_{||}/\mu_{\perp}$, was reported to be 5−8 for F8T2 and 8 for P3DDT. These values are comparable to that of our experimental results. The anisotropy factor was evaluated at 6, 9, and 11 for F(MB)-10F(EH)2, F(Pr)5F(MB)2, and PFO, respectively. This is opposite to the trend in R_{abs}, a consequence of the interplay between two factors: how chain or persistence length affects $\mu_{||}$ and how the aliphatic pendant structure affects $\mu_{\perp}$. Grell, et al. reported a persistence length of 8.5 nm for PFO in dilute solution.[34] For F(Pr)5F(MB)2 and F(MB)10F(EH)2, the extended oligomer length was estimated by molecular simulation (MM2, Alchemy) at 5.9 and 10.1 nm, respectively. It is anticipated that the longer the oligofluorene's extended length, without incurring intrachain defects, or the polyfluorene's persistent length, the higher the $\mu_{||}$ value because of the lesser number of interchain hops over the same FET channel length. The observed trend in $\mu_{||}$, F(MB)-10F(EH)2 > PFO > F(Pr)5F(MB)2, suggests that both hepta- and dodecafluorenes are devoid of chain defects, thus ensuring the advantage of oligomers at a critical chain length.

(33) Nagamatsu, S.; Takashima, W.; Kaneto, K.; Yoshida, Y.; Tanigaki, N.; Yase, K. *Appl. Phys. Lett.* **2004**, *84*, 4608.

(34) Grell, M.; Bradley, D. D. C.; Long, X.; Inbasekaran, M.; Woo, E. P.; Soliman, M. *Acta Polym.* **1998**, *49*, 439.

Table 1. Hole Mobility in OFETs Parallel ($\mu_{||}$) and Perpendicular ($\mu_{\perp}$) to the Rubbing Direction of Monodomain Glassy-Nematic Films, in Polydomain Glassy-Nematic Films ($\mu_{\times}$), and in Glassy-Amorphous Films (μ_a)

	$\mu_{||}$ (cm^2/Vs)	$\mu_{\times}$ (cm^2/Vs)	$\mu_{\perp}$ (cm^2/Vs)	μ_a (cm^2/Vs)
F(MB)10F(EH)2	$1.2 \pm 0.2 \times 10^{-2}$	$5.1 \pm 0.3 \times 10^{-3}$	$1.9 \pm 0.1 \times 10^{-3}$	$1.5 \pm 0.3 \times 10^{-5}$
F(Pr)5F(MB)2	$1.7 \pm 0.4 \times 10^{-3}$	$7.8 \pm 1.8 \times 10^{-4}$	$1.9 \pm 0.1 \times 10^{-4}$	$2.1 \pm 1.1 \times 10^{-5}$
PFO	$5.8 \pm 0.7 \times 10^{-3}$	$2.2 \pm 0.3 \times 10^{-3}$	$5.2 \pm 0.5 \times 10^{-4}$	$3.3 \pm 0.5 \times 10^{-4}$

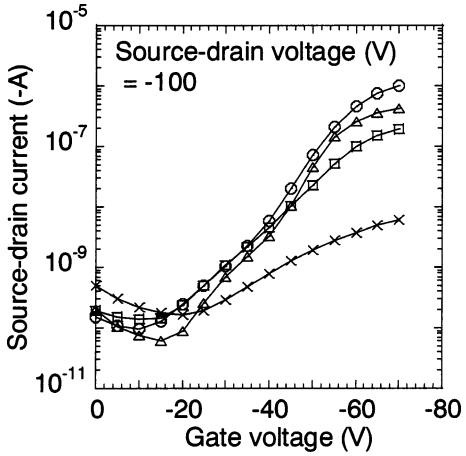

Figure 6. Transfer characteristics at $V_D = -100$ V of an OFET comprising a monodomain glassy-nematic F(MB)10F(EH)2 film parallel (○) and perpendicular (□) to the rubbing direction, and those of OFETs comprising a polydomain glassy-nematic (△) and a glassy-amorphous (×) F(MB)10F-(EH)2 film.

Above this critical chain length, there is sufficient overlap between neighboring chains to enable interchain hopping beyond intrachain charge transport. Nevertheless, the oligomer length cannot be increased indefinitely without encountering chain entanglement, bends, and kinks that have an adverse effect on mobility. For lack of information on intermolecular packing in the presence of disparate aliphatic pendant structures and on the roughness perpendicular to the rubbing direction, it is impossible to offer an interpretation of the observed trend in $\mu_{\perp}$ at this time.

Two other general observations are noted for the three materials: $\mu_{||} > \mu_{\times} > \mu_{\perp}$ and $\mu_{\perp} > \mu_a$. That $\mu_{\times} > \mu_{\perp}$ can be interpreted in terms of $\mu_{\perp}$ in a monodomain film being contributed exclusively by interchain hopping whereas $\mu_{\times}$ in a polydomain film being facilitated in part by intrachain transport along the FET channel. Glassy-amorphous films presented the least mobility of all presumably because of the geometric and energetic disorder. The trend in $\mu_{||}$, as established above, and that in μ_a, PFO > F(Pr)5F(MB)2 ≈ F(MB)10F(EH)2, lead to the mobility enhancement in monodomain glassy-nematic films over glassy-amorphous films, $\mu_{||}/\mu_a = 800$, 81, and 18 for F(MB)10F(EH)2, F(Pr)-5F(MB)2, and PFO, respectively.

Summary

Field-effect transistors were fabricated using hepta- and dodecafluorenes, F(Pr)5F(MB)2 and F(MB)10F(EH)2, and a polyfluorene. Hole mobilities were measured for devices comprising monodomain and polydomain glassy-nematic films as well as glassy-amorphous films. Oligofluorenes were more readily aligned into monodomain films via thermal annealing at a lower temperature, resulting in a higher R_{abs} than polyfluorene. Glassy-amorphous films possess the lowest mobility of all because of the geometric and energetic disorder. The mobility of a monodomain glassy-nematic F(MB)10F(EH)2 film is enhanced over that of a glassy-amorphous film by a factor of 800. In monodomain films, the $\mu_{||}$ value is determined by the oligofluorene's chain length and the polyfluorene's persistence length. For F(MB)10F-(EH)2, $\mu_{||}$ was evaluated at 0.012 cm^2/Vs with an on/off ratio of 1.0×10^4. This mobility value is twice that of polyfluorene in the same device structure. It is concluded that monodisperse glassy-nematic conjugated oligomers hold great potential for use in field-effect transistors because of their superior chemical purity, structural uniformity and regularity, and ease of processing into uniaxially aligned defect-free films.

Acknowledgment. T.T. thanks Daisankasei Co. Ltd. for providing the starting material of poly-chloro-*p*-xylylene and funding from the Ministry of Education, Science, Sports and Culture, Grant-in-Aid for Scientific Research (B), 16360011, 2004. S.H.C. acknowledges funding from the U. S. National Science Foundation, Army Research Office, Department of Energy, Eastman Kodak Company, and the New York State Center for Electronic Imaging Systems.

CM048532S